Numerical Simulation of a PSA System

Part I: Isothermal Trace Component System with Linear Equilibrium and Finite Mass Transfer Resistance

A numerical simulation of a pressure swing adsorption process is presented for a system in which a small concentration of an adsorbable component is separated from an inert carrier. Linear equilibrium and a linear rate expression are assumed. The model equations were solved by orthogonal collocation and by finite difference methods with consistent results. The theory is shown to provide a good representation of the experimental data of Mitchell and Shendalman (1973) for the system CO_2-He-silica gel.

N. S. RAGHAVAN, M. M. HASSAN, and D. M. RUTHVEN

Department of Chemical Engineering
University of New Brunswick
Fredericton, NB, Canada

SCOPE

A pressure swing adsorption (PSA) system has been simulated using both the finite difference method and the method of orthogonal collocation to solve the model equations. It is shown that axial dispersion has a greater effect on the cyclic steady-state profile in a PSA system than in a single stage fixed bed; the effects of various combinations of Peclet number and mass transfer resistance are also investigated. The theoretically predicted behavior of the system is compared with the experimental data of Mitchell and Shendalman (1973) for separation of CO_2-He mixture on silica gel.

CONCLUSIONS AND SIGNIFICANCE

The solutions for the cyclic steady state profiles obtained by finite difference and collocation methods agree well, but the collocation method requires much less computer time for similar accuracy. The cyclic steady-state concentration profile is sensitive to a linear combination of Peclet number and mass transfer resistance, but not to the individual values of these parameters. If it is assumed that the effective mass transfer coefficient is inversely dependent on total pressure, as is to be expected if external film or pore diffusional resistance in the molecular diffusion regime is the dominant resistance, a good fit of the experimental data of Mitchell and Shendalman (1973) is obtained.

INTRODUCTION

Since the initial development of the heatless drier (Skarstrom, 1959, 1960, 1972) pressure swing adsorption (PSA) processes have gained increasing industrial importance and are now used to carry out several commercially important separations, including hydrogen purification and air separation, as well as drying. In a PSA process the raffinate product (the least strongly adsorbed species) can be recovered at high purity but only at relatively low fractional recovery. Such processes are therefore most useful for the separation of mixtures in which the feed is relatively inexpensive and the required product is the less strongly adsorbed species. These conditions are fulfilled by all three processes referred to above.

The performance of a PSA system is controlled by process variables such as the bed length, flow velocity, pressure ratio, and purge/feed ratio, as well as by the basic kinetic and equilibrium relationships for the particular system. The effects of the process variables are coupled and therefore difficult to visualize, making it hard to achieve an optimal design by the intuitive approach. A reliable mathematical simulation which provides an adequate representation of the system dynamics is therefore required.

Despite the widespread and increasing application of such processes, the problem of developing a suitable mathematical simulation has not yet been fully solved. Shendalman and Mitchell (1972) developed the basic equilibrium theory model for sorption of a trace concentration of an adsorbable species from an inert carrier, subject to the assumptions of plug flow and linear equilibrium. In a more recent version of the equilibrium theory (Chan et al., 1981) the analysis was extended to include adsorption of the carrier, but the assumption that the more strongly adsorbed species is present only at trace concentration was retained. This restriction has now been relaxed and the general equilibrium theory for a system with two adsorbable species present at any concentration level was given by Knaebel and Hill (1982).

N. S. Raghavan is presently at ALCAN International Ltd., Kingston, Ontario, Canada.

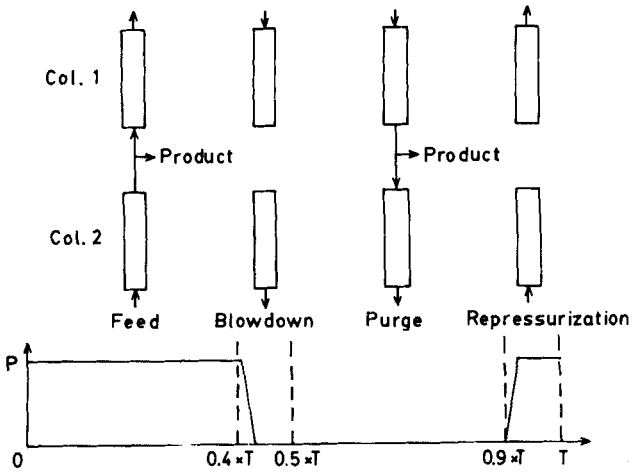

Figure 1. Schematic representation of steps in a PSA cycle.

Such an analysis provides valuable information concerning the minimum purge/feed ratio and column length required to produce a pure raffinate product for any specified separation factor and pressure ratio. However, in real systems dispersive effects (finite mass transfer resistance and axial dispersion) are generally important, so that equilibrium theory provides only a crude guide to performance. In order to obtain a more realistic model these effects must be included.

A dynamic model including finite mass transfer resistance but not axial dispersion was developed by Mitchell and Shendalman (1973), but was found to provide only a poor representation of the experimental data obtained in a study of the separation of a CO_2-He mixture in a small laboratory PSA system. A somewhat similar model was developed by Chihara and Suzuki (1981) who included also the heat balance equations to allow for nonisothermal operation.

The numerical calculations involved in the solution of the differential equations describing the dynamic behaviour of a PSA system are bulky, because in order to determine the cyclic steady state it is necessary to repeat the computations for approximately 30–40 cycles. However, the number of cycles required to reach the steady state may be somewhat fewer in the case of partially loaded beds. Efficient numerical methods are therefore essential. Previous dynamic models have used standard finite difference methods, but in the simulation of the performance of a single adsorption column, collocation methods often have been found to be superior in that the computing time required to obtain a solution of specified accuracy is substantially reduced (Santacesaria et al., 1982; Raghavan and Ruthven, 1983). In the present study, which was undertaken as the first step toward the development of a general dynamic model for an air separation PSA unit, the collocation method was therefore employed. We have included both axial dispersion and mass transfer in the mathematical model but in order to simplify the problem we have assumed isothermal behavior, which is a valid approximation when the concentration of the adsorbable species is small.

MATHEMATICAL MODEL

The basic PSA cycle involves four distinct steps as indicated in Figure 1. During step 1 a high pressure feed is supplied continuously to bed 2 in which preferential adsorption of the more strongly adsorbed component occurs. The less strongly adsorbed species is removed as pure raffinate product at the bed outlet. A small fraction of this stream is expanded to low pressure and used to purge bed 1. In step 2, bed 1 is pressurized with feed while bed 2 is blown down in the reverse flow direction. The same cycle is repeated in steps 3 and 4 with bed 1 being pressurized and bed 2 purged. In order to develop a mathematical model for this system the following approximations are introduced:

(1) The feed consists of a small concentration of a single adsorbable component in an inert carrier.

(2) The system is isothermal with negligible pressure drop through the adsorbent beds.

(3) The pressure change in steps 2 and 4 is so rapid that no significant exchange between adsorbed and gas phases occurs during pressurization or blowdown.

(4) The equilibrium relationship is linear.

(5) The flow pattern is described by the axial dispersed plug flow model.

(6) The mass transfer rate is represented by a linear driving force expression.

Assumptions 1 and 2 imply a constant linear velocity through the adsorbent bed, but the magnitude of this velocity will generally be different for adsorption and desorption steps. Axial dispersion in a packed bed may be represented approximately by:

$$D_L \approx \gamma_1 D_m + \gamma_2 ud \tag{1}$$

where γ_1 and γ_2 are constants having values of approximately 0.7 and 0.5 respectively. At high Reynolds number the axial Peclet number (uL/D_L) is independent of either pressure or gas velocity and is therefore the same for the adsorption (high pressure) and desorption (low pressure purge) steps. At low Reynolds number the axial Peclet number is given approximately by $uL/D_L \approx uL/0.7D_m$. Since the molecular diffusivity is inversely proportional to total pressure and, for a given molar flow rate the gas velocity is also inversely proportional to pressure, the Peclet number is independent of pressure but depends on the molar flow rate. The ratio of the Peclet numbers for the adsorption and desorption steps is therefore given simply by the molar feed/purge ratio.

The mass transfer coefficient may be different for the high pressure and low pressure steps. If the controlling resistance is macropore diffusion in the molecular regime $k\alpha D_m \alpha 1/P$ while within the Knudsen regime or under conditions of micropore control, the mass transfer coefficient will be effectively independent of pressure and therefore the same for adsorption and desorption steps.

This model is similar to the model of Mitchell and Shendalman (1973) except that axial dispersion is included and the effect of pressure on the mass transfer coefficient is allowed for. Subject to these approximations the dynamic behavior of the system may be described by the following set of equations.

Step 1

High pressure flow in bed 2 and low pressure (purge) flow in bed 1.

External Fluid

$$\text{Bed 2:}\quad -D_{L_2}\frac{\partial^2 C_2}{\partial z^2} + u_2\frac{\partial C_2}{\partial z} + \frac{\partial C_2}{\partial t} + \frac{(1-\epsilon)}{\epsilon}\cdot\frac{\partial q_2}{\partial t} = 0 \tag{2}$$

$$\text{Bed 1:}\quad -D_{L_1}\frac{\partial^2 C_1}{\partial z^2} + u_1\frac{\partial C_1}{\partial z} + \frac{\partial C_1}{\partial t} + \frac{(1-\epsilon)}{\epsilon}\cdot\frac{\partial q_1}{\partial t} = 0 \tag{3}$$

Mass Transfer Rate Expression

$$\text{Bed 2:}\quad \frac{\partial q_2}{\partial t} = k_2(q_2^* - q_2) \tag{4}$$

$$\text{Bed 1:}\quad \frac{\partial q_1}{\partial t} = k_1(q_1^* - q_1) \tag{5}$$

Adsorption Equilibrium

$$\text{Bed 2:}\quad q_2^* = KC_2 \tag{6}$$

$$\text{Bed 1:}\quad q_1^* = KC_1 \tag{7}$$

Boundary Conditions

$$\text{Bed 2:}\quad D_{L_2}\left.\frac{\partial C_2}{\partial z}\right|_{z=0} = -u_2(C_2|_{z=0^-} - C_2|_{z=0}) \tag{8}$$

$$\left.\frac{\partial C_2}{\partial z}\right|_{z=L} = 0 \tag{9}$$

$$\text{Bed 1:}\quad D_{L_1}\left.\frac{\partial C_1}{\partial z}\right|_{z=0} = -u_1\left(\frac{P_L}{P_H}\cdot C_z - C_1|_{z=0}\right) \tag{10}$$

$$\left.\frac{\partial C_1}{\partial z}\right|_{z=L} = 0 \tag{11}$$

Note that in Eq. 10 C_z is the exit concentration of bed 2 during step 1. As a result of the pressure reduction the inlet concentration for the desorption step is therefore given by $(P_L/P_H)C_z$.

Initial Conditions

$$C_2(z,0) = 0;\quad q_2(z,0) = 0;\quad C_1(z,0) = 0;\quad q_1(z,0) = 0 \tag{12}$$

As a consequence of assumption 3, the solid phase concentration is assumed frozen during pressurization and blowdown and the solid concentration profile is therefore the same at the start of desorption as at the end of the adsorption step. The gas phase concentration at the end of the pressurization step is assumed to be uniform through the bed and equal to the feed concentration. The blowdown is described by the following equations:

Step 2 for Bed 2

External Fluid

$$-D_{L_2}\frac{\partial^2 C_2}{\partial z^2} - \frac{\partial(uC_2)}{\partial z} + \frac{\partial C_2}{\partial t} = 0 \tag{13}$$

Overall Continuity

$$\frac{\partial u}{\partial z} = \frac{1}{P}\cdot\frac{\partial P}{\partial t} \tag{14}$$

Boundary Conditions

$$\left.\frac{\partial C_2}{\partial z}\right|_{z=0} = 0;\quad \left.\frac{\partial C_2}{\partial z}\right|_{z=L} = 0;\quad u|_{z=L} = 0 \tag{15}$$

The blowdown of bed 1 occurs during step 4, and the relevant equations are

$$-D_{L_1}\frac{\partial^2 C_1}{\partial z^2} + \frac{\partial(uC_1)}{\partial z} + \frac{\partial C_1}{\partial t} = 0$$

$$-\frac{\partial u}{\partial z} = \frac{1}{P}\frac{\partial P}{\partial t}$$

$$\left.\frac{\partial C_1}{\partial z}\right|_{z=0} = 0;\quad \left.\frac{\partial C_1}{\partial z}\right|_{z=L} = 0;\quad u|_{z=0} = 0$$

The initial condition is the concentration profile at the end of the preceding high pressure (adsorption) step.

These equations were written in dimensionless form and solved to give the concentration profiles through the bed (C/C_o and q/KC_o) as a function of dimensionless distance (z/L) and the dimensionless time variable $\tau = u_2 t/L$ with the following parameters:

$$Pe_H = \frac{u_2 L}{D_{L_2}},\quad Pe_L = \frac{u_1 L}{D_{L_1}},\quad \alpha = \frac{u_1}{u_2},\quad \tau_{fH} = \frac{k_2 L}{u_2},$$

$$\tau_{fL} = \frac{k_1 L}{u_2};\quad Y_D = \frac{L}{u_2 t_B}\ln\left(\frac{P_L}{P_H}\right)$$

where t_B is the blowdown time. In most of the computations we have assumed $D_L \alpha u$ and $k\alpha 1/P$, but to investigate the effects of these assumptions a few calculations were made with k constant and $D_L \alpha 1/P$. The dimensionless time for blowdown was set arbitrarily at one-quarter of the half-cycle time. A limited investigation revealed that provided this time was at least one-tenth of the half-cycle time it had no effect on the profile, so the assumption $t_B = 0.25t^*$ is in no way critical.

The solution to the dimensionless model equations was obtained by both collocation and finite difference methods; brief details are given in the appendix. For the collocation solution 15 collocation points were found necessary to obtain an accurate solution, while for the finite difference solution the bed was divided into 30 spatial intervals in order to generate solutions of comparable accuracy. However, it is to be noted that Chihara and Suzuki (1983) employed 40 spatial intervals in their finite difference approach to solve the same set of equations.

TABLE 1. COMPARISON OF RESULTS COMPUTED BY COLLOCATION AND BY FINITE DIFFERENCE (3 POINT CENTRAL)

Cycle No.	Exit Concentration at the End of High Pressure Step in Bed 2: Collocation Method with 15 Collocation Points	Finite Diff. with 30 Spatial Intervals
10	0.007528	0.006032
20	0.014153	0.011937
30	0.020682	0.017677
35	0.022609	0.019924
Computation Time Required	15 min	45 min

The simulation for this comparison were carried out for the parameters $Pe_H = Pe_L = 10^3$ $\alpha = 2.0$, $L = 0.5$ m, $t^* = 270$ s, $K = 9084$, $k_2 = 2.78 \times 10^{-4}$ s^{-1}, $u_2 = .25$ m/s, $P_H = 5.07 \times 10^5$ (Pa), $P_L = 1.01 \times 10^5$ (Pa), $\epsilon = 0.4$. These are representative of a heatless drier system.

RESULTS OF NUMERICAL SIMULATION

In order to examine the effects of the process variables (Peclet number, purge/feed ratio, column length, and cycle time) on the performance of the system and to compare the collocation and finite difference solutions the parameters used by Chihara and Suzuki (1981) for a heatless drier (moist air–alumina) were used. The results are summarized in Table 1 and Figures 2a and 2b, which show the fluid phase concentration profiles at the end of the adsorption (high pressure) and purge (low pressure) steps. An initially clean bed was assumed at the start of the first cycle and the progress toward the cyclic steady-state profile, which is reached

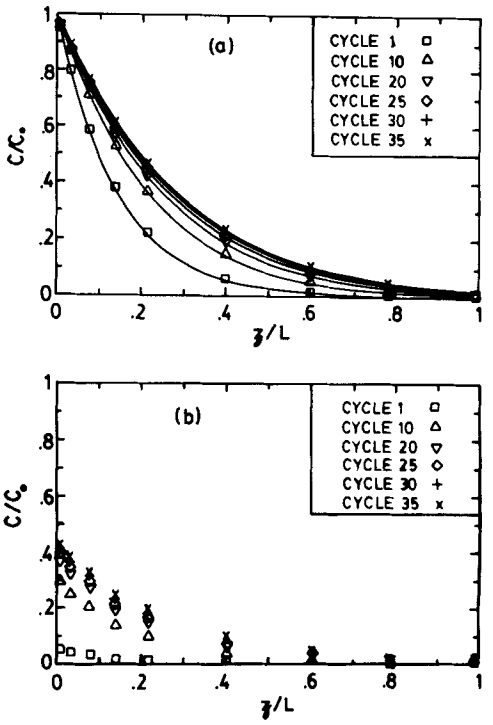

Figure 2. (a) Gas phase concentration profiles at end of high pressure (adsorption) step. (b) Gas phase concentration profiles at end of low pressure (desorption or purge) step, showing progress toward cyclic steady state for a system with parameters specified in Table 1.

($Pe_H = Pe_L = 10^3$; $\alpha = 2.0$, $\tau_{fH} = 5.56 \times 10^{-4}$; $K = 9084$).

TABLE 2. COMPARISON OF OUTLET CONCENTRATIONS AT END OF ADSORPTION CYCLE FOR STEADY STATE CYCLIC OPERATION SHOWING EFFECT OF PROCESS VARIABLES

Except where specified, $Pe_H = Pe_L$ or $D_L\alpha u$, and $k\alpha 1/P$.

Variable Effect	Constant Parameters Values	Variable Parameter Values	$C_2/C_o\|_{x=1}$ When $k\alpha 1/P$	$C_2/C_o\|_{x=1}$ When k Const.
Effect of Axial Dispersion	$\alpha = 2.0$ $L = 0.5$ m $t^* = 270$ s	$D_L\alpha u$ $Pe_H = 10$	0.0838	0.1087
		$D_L\alpha 1/P$ $Pe_H = 10$	0.1097	0.1200
		$Pe_H = 100$	0.0281	0.0515
		$Pe_H = 1{,}000$	0.0226	—
Effect of Purge to Feed Ratio	$Pe_H = 1{,}000$ $L = 0.5$ m $t^* = 270$ s	$\alpha = 2.0$	0.0226	
		$\alpha = 3.0$	0.0198	
Effect of Bed Length	$Pe_H = 1{,}000$ $\alpha = 2.0$	$L = 0.5$ m $t^* = 270$ s	0.0226	
		$L = 1.0$ m $t^* = 270$ s	0.0016	
Effect of Cycle Time	$Pe_H = 1{,}000$ $\alpha = 2.0$ $L = 0.5$ m	$t^* = 270$ s	0.0226	
		$t^* = 135$ s	0.0139	

after about 35 cycles, is clearly apparent. The outlet concentration for bed 2 at the end of the 10th, 20th, 30th and 35th cycles are compared in Table 1. The solutions obtained by the two methods are broadly consistent but the computer time required for the finite difference calculation was about three times as long as for the collocation solution.

The effects of the process variables are summarized in Table 2. The effects of cycle time, bed length, and purge/feed ratio are as expected. Provided that the purge is sufficient to remove most of the gas phase from the interstices of the bed ($\alpha > \sim 1.5$) a further increase has only a minor effect on product purity. The most striking result is the effect of axial dispersion. Simulation of a single adsorbent bed subjected to a step change in sorbate concentration at the inlet shows that, with the same parameter values as used in example 1 of Table 2, the effect of axial dispersion on the concentration profile becomes insignificant for $Pe > 100$ (Figure 3a). By contrast, at this level the cyclic steady state profile in the PSA system is still significantly affected by axial dispersion and the effluent concentration at the end of the high pressure step decreases from 2.8% to 2.2% as the Peclet number increases from 100 to 1,000 (Figure 3b). It is evident that the effect of axial dispersion in broadening the concentration profile is in some sense cumulative from cycle to cycle.

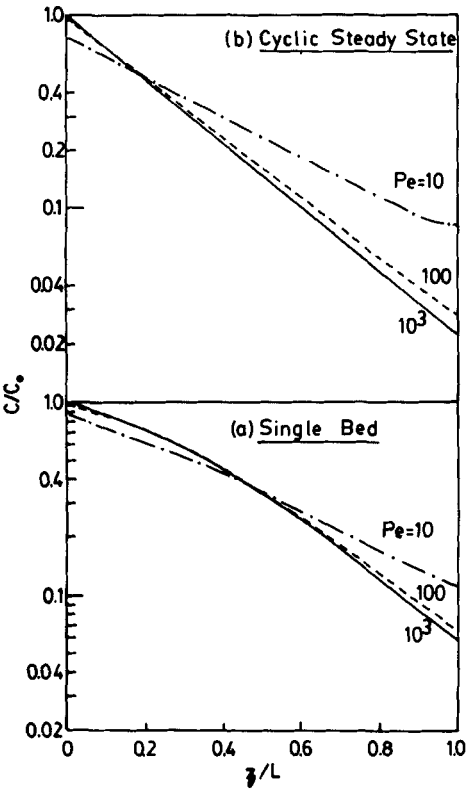

Figure 3. (a) Concentration profile at breakthrough for a single adsorbent bed subjected to a step change in sorbate concentration at the inlet. (b) cyclic steady state concentration profile at the end of adsorption step, showing effect of *Pe*. Parameters for (a) and (b) are as defined in Table 2, example 1.

Both cases when $D_L\alpha u$ and $D_L\alpha 1/P$ have been considered. No significant changes were observed at high Peclet number, but at low Peclet number the steady state exit concentration of the adsorbable component was found to increase on going from the high Reynolds number regime ($D_L\alpha u$) to low Reynolds number regime ($D_L\alpha 1/P$), the effect being more pronounced when $k\alpha 1/P$ as seen from Table 2. The increase in the total resistance $(1/Pe + \epsilon u/(1 - \epsilon)LkK)$ for the desorption step is responsible for these effects.

It is well-known from the analysis of chromatographic data that for a single adsorption column, axial dispersion and finite resistance to mass transfer exert similar effects in broadening the concentration profile. This appears to be true also for a PSA system at cyclic steady state. Eqs. 2-15 were solved (with $Pe_H = Pe_L$ and $k\alpha 1/P$) for a series of different values of Pe and k such that the linear combination $(1/Pe) + [\epsilon u/(1 - \epsilon)kKL]$ for high pressure flow step remains constant. The results are summarized in Figure 4. It is evident that the steady state concentration profile is not sensitive to the individual values of Pe and kL/u but only to the linear combination. The extreme case of $kL/u \to \infty$ corresponds to a system in which equilibrium is always established between gas and solid while $Pe \to \infty$ corresponds to plug flow with finite mass transfer resistance.

COMPARISON WITH EXPERIMENTAL DATA

An experimental study of the PSA separation of CO_2-He on silica gel was reported by Mitchell and Shendalman (1973); their data for three representative runs are shown in Figure 5 together with the curves calculated from the theoretical model with the parameters given in Table 3. Initially both beds were assumed to be at equilibrium with the feed at their respective operating pressures since this was the initial condition used in the experiments. All parameters except the Peclet number and mass transfer resistance may be calculated directly from the experimental conditions. The

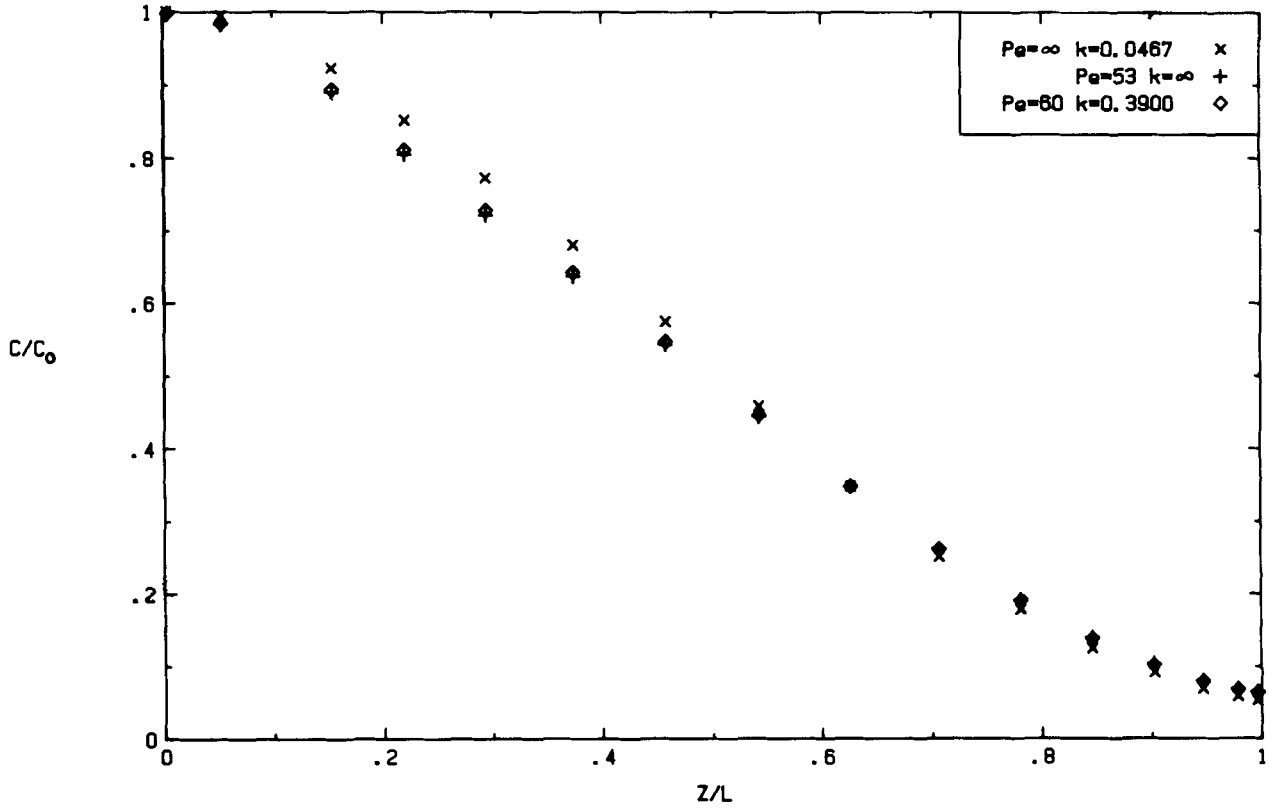

Figure 4. Comparison of cyclic steady state profiles for different values of *Pe* and *kL/u* such that $1/Pe + [\epsilon u/(1-\epsilon)LkK]$ remains constant. Other parameter values are as given in Table 3, Run 9.

overall mass transfer coefficient was determined by Mitchell and Shendalman from analysis of an experimental breakthrough curve measured under high pressure flow conditions ($k = 0.0467\ s^{-1}$). If we assume the controlling mass transfer resistance to be intraparticle diffusion rather than external film resistance, the mass transfer coefficient should be independent of velocity and therefore constant for all runs carried out at the same temperature and pressure. This value of mass transfer coefficient which was derived assuming plug flow ($D_L \to \infty$) should more properly be considered as defining the linear combination $[1/Pe + \epsilon u/(1-\epsilon)kKL]$, and the corresponding values of this parameter for the three experimental runs are given in Table 3. In calculating the theoretical curves we have assumed $k\alpha 1/P$ so that the resistance is substantially different for the adsorption and desorption cycles.

It is evident from Figure 5 that these theoretical curves provide a good representation of the experimental results with the same mass transfer and dispersion coefficients for all three runs. However, it is not possible to resolve the linear combination and assign individual values to the mass transfer coefficient and Peclet number. Also shown in Figure 5 are the theoretical curves calcu-

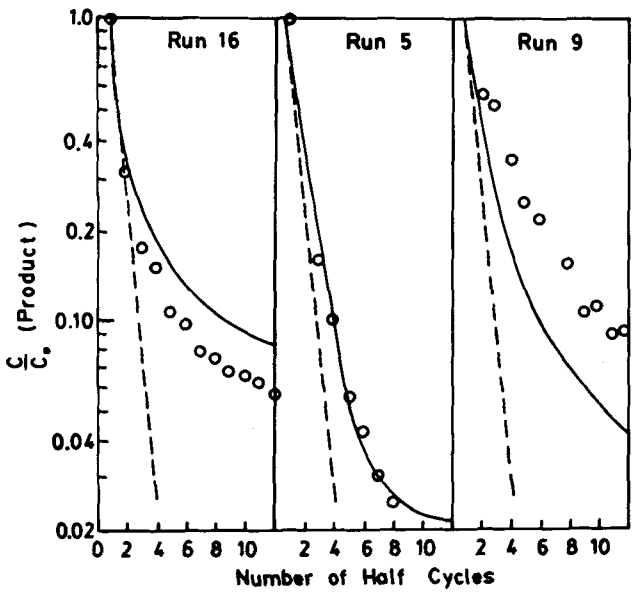

Figure 5. Comparison of experimental data of Mitchell and Schendalman (1973) with prediction of theoretical model. O Expt., M&S (1973); - - - Theoretical, M&S (1973); — Present Model.

TABLE 3. PARAMETERS USED IN CALCULATION OF THEORETICAL CURVES FOR DATA OF SHENDALMAN AND MITCHELL (FIGURE 5)

Common Parameters	
Feed Gas Composition	1.09% CO_2 in He
Feed Pressure	4.0 atm†
Purge Pressure	1.33 atm†
Column Length	61 cm
Cross Section Area	11.4 cm^2
Bed Porosity	0.42
Adsorption Equilibrium Constant K (Dimensionless)	52.7
Time for Steps 2 and 4	0.25 t*
Temperature	25°C
Adsorbent	W. R. Grace Silica Gel (Tel-Tale, grade 92, 6–16 mesh)

Parameters for Individual Runs			
Parameter	Run 5	Run 9	Run 16
$\alpha = u_1/u_2$	1.5	1.5	1.08
Feed Rate (SCFM)	0.0363	0.15	0.038
Time for Steps 1 and 3 t* (sec)	720	180	720
Dimensionless time for steps 1 and 3 t^*u_2/L	10.56	10.91	11.05
Linear Combination $[1/Pe + \epsilon u_2/(1-\epsilon)kKL]$	10.56	0.0188	0.0055
k‡ (sec^{-1})	0.0467	0.0467	0.0467

† SI conversion: atm × 101.3 = kPa.
‡ Values of k at high pressure assuming $Pe \to \infty$. It is assumed that $k\alpha 1/p$.

lated according to equilibrium theory assuming plug flow and negligible axial dispersion. It is evident that these curves do not fit the experimental data.

The key difference between the present model which provides a good fit of the experimental data and the model of Mitchell and Shendalman (1973) which gave a poor representation, lies in the assumption that the mass transfer coefficient varies inversely with the pressure. Such behavior is to be expected for a system in which the uptake is controlled by film or macropore diffusional resistance in the molecular diffusion regime and therefore appears reasonable for this system, but it has not been confirmed directly by experiment.

The present simulation with the assumption of frozen solid-phase concentration during blowdown and pressurization should provide a useful model for PSA separations involving an adsorbable component in trace amounts. However, a more thorough investigation which would allow for velocity variation and solid phase concentration changes during blowdown and pressurization steps may be necessary for systems involving bulk gas separations such as air in carbon molecular sieves and synthetic zeolites.

APPENDIX

When we consider the high pressure flow in bed 2 and the low pressure flow in bed 1 as the operations during Step 1, the relevant equations for bed 2 are, Eq. 2, 4, 6, 8, and 9, and those which describe the operation in bed 1 are Eqs. 3, 5, 7, 10, and 11.

Since steps 1 and 3 are identical except for the direction of flow, it is sufficient to consider the equations relevant to step 1.

Equations 2, 4, and 6 combined and written in dimensionless form become:

$$\frac{\partial \bar{C}_2}{\partial \tau} = \frac{1}{Pe_H}\frac{\partial^2 \bar{C}_2}{\partial x^2} - \frac{\partial \bar{C}_2}{\partial x} - m \cdot K \cdot \tau_{fH}(\bar{C}_2 - \bar{q}_2) \tag{16}$$

Equations 4 and 6 combined and in dimensionless form yield

$$\frac{\partial \bar{q}_2}{\partial \tau} = \tau_{fH}(\bar{C}_2 - \bar{q}) \tag{17}$$

The relevant boundary conditions, Eqs. 8 and 9 in dimensionless form lead to

$$\left.\frac{\partial \bar{C}_2}{\partial x}\right|_{x=0} = -Pe_H(\bar{C}_2|_{x=0^-} - \bar{C}_2|_{x=0}) \tag{18}$$

$$\left.\frac{\partial \bar{C}_2}{\partial x}\right|_{x=1} = 0 \tag{19}$$

Similarly, for bed 1 the following dimensionless equations are arrived at based on Eqs. 3, 5, 7, 10, and 11:

$$\frac{\partial \bar{C}_1}{\partial \tau} = \alpha\frac{1}{Pe_L}\frac{\partial^2 \bar{C}_1}{\partial x^2} - \alpha\frac{\partial \bar{C}_1}{\partial x} - m \cdot K \cdot \tau_{fL}(\bar{C}_1 - \bar{q}_1) \tag{20}$$

$$\frac{\partial \bar{q}_1}{\partial \tau} = \tau_{fL}(\bar{C}_1 - \bar{q}_1) \tag{21}$$

$$\left.\frac{\partial \bar{C}_1}{\partial x}\right|_{x=0} = -Pe_L(G \cdot \bar{C}_2|_{x=1 \text{ of bed } 2} - C_1|_{x=0}) \tag{22}$$

$$\left.\frac{\partial \bar{C}_1}{L\partial x}\right|_{x=1} = 0 \tag{23}$$

where

$$G = P_L/P_H$$

Equation 12, which is a valid condition for the startup of the cyclic operation with two clean beds, leads to the following two sets of dimensionless equations:

$$\bar{C}_2(x,\tau = 0) = 0; \quad \bar{q}_2(x,\tau = 0) = 0 \tag{24}$$

$$\bar{C}_1(x,\tau = 0) = 0; \quad \bar{q}_1(x,\tau = 0) = 0 \tag{25}$$

Just as in the case of steps 1 and 3, steps 2 and 4 are identical except for the location of the closed end of the column. Therefore, in what follows we discuss the equations for bed 2 with step 2 in mind.

Equation 14 can be written in dimensionless form as

$$-\frac{1}{\bar{P}} \cdot \frac{\partial \bar{P}}{\partial \tau} = \frac{\partial U}{\partial x} \tag{26}$$

where

$$\bar{P} = P/P_H, \quad U = u/u_2$$

After making the assumption that $\partial U/\partial x = y_D$ and integrating the above, that is,

$$-\int_{\bar{P}=\bar{P}_H}^{\bar{P}=\bar{P}_L} \frac{\partial \bar{P}}{\bar{P}} = y_D \int_0^{\tau=\tau_b} \partial\tau$$

we get,

$$y_D = \frac{1}{\tau_b} \ln \frac{1}{\bar{P}_L}$$

where

$$\bar{P}_H = 1, \quad \bar{P}_L = P_L/P_H \text{ and } \tau_b = t_b u_2/L$$

Since,

$$\left.\begin{aligned} \frac{\partial U}{\partial x} &= y_D \text{ (constant)} \\ U &= y_D(x - 1) \end{aligned}\right\} \tag{27}$$

Equation 13 when written in dimensionless form therefore becomes,

$$\frac{\partial \bar{C}_2}{\partial \tau} = \frac{1}{Pe_H}\frac{\partial^2 \bar{C}_2}{\partial x^2} + y_D(x - 1)\frac{\partial \bar{C}_2}{\partial x} + \bar{C}_2 y_D \tag{28}$$

The boundary conditions specified in Eq. 15 when rendered dimensionless become:

$$\left.\frac{\partial \bar{C}_2}{L\partial x}\right|_{x=0} = 0; \quad \left.\frac{\partial \bar{C}_2}{L\partial x}\right|_{x=1} = 0; \quad U|_{x=1} = 0 \tag{29}$$

When Eqs. 16, 18, and 19 are combined and written in collocation form based on a Legendre type polynomial to represent the trial function (Villadsen and Stewart (1967), Finlayson (1972)), the following set of ordinary differential equations result for the high pressure flow step in bed 2 (step 1):

$$\begin{aligned} \frac{d\bar{C}_2}{d\tau}(j) = \Bigg[& \sum_{i=2}^{M+1} [P \cdot Bx(j,i) - Ax(j,i)] - A_4 \cdot [P \cdot Bx(j,1) - Ax(j,1)] \cdot \sum_{i=2}^{M+1} Ax(M+2,i) \\ & - A_5 \cdot [P \cdot Bx(j,1) - Ax(j,1)] \cdot \sum_{i=2}^{M+1} [A_3 \cdot Ax(M+2,i) - Ax(1,i)] \\ & + A_1 \cdot [P \cdot Bx(j,M+2) - Ax(j,M+2)] \cdot \sum_{i=2}^{M+1} [A_3 \cdot Ax(M+2,i) - Ax(1,i)] \Bigg] \cdot \bar{C}_2(i) \\ & + A_5 \cdot Pe_H \cdot \bar{C}_2|_{x=0^-} \cdot [P \cdot Bx(j,1) - Ax(j,1)] \\ & - A_1 \cdot Pe_H \cdot \bar{C}_2|_{x=0^-} \cdot [P \cdot Bx(j,M+2) - Ax(j,M+2)] \\ & - m \cdot K \cdot \tau_{fH} \cdot [\bar{C}_2(j) - \bar{q}_2(j)] \end{aligned} \tag{30}$$

Equation 17 now becomes,

$$\frac{d\bar{q}_2}{d\tau}(j) = \tau_{fH} \cdot [\bar{C}_2(j) - \bar{q}_2(j)] \qquad j = 2, \quad M+1 \qquad (31)$$

In equation 30,

$$A_1 = 1/\{Ax(1,M+2) - [A_3 \cdot Ax(M+2,M+2)]\}$$

$$A_2 = Ax(M+2,M+2)/\{Ax(1,M+2) - [A_3 \cdot Ax(M+2,M+2)]\}$$

$$A_3 = [Ax(1,1) - Pe_H]/Ax(M+2,1)$$

$$A_4 = 1/Ax(M+2,1)$$

$$A_5 = A_2 \cdot A_4$$

$$P = 1/Pe_H$$

M = Number of collocation points

Equations 20, 22, and 23, combined and transformed into ODE's by the collocation method lead to:

$$\frac{d\bar{C}_1}{d\tau}(j) = \left[\sum_{i=2}^{M+1} [Q \cdot Bx(j,i) - \alpha \cdot Ax(j,i)] - B_4 \cdot [Q \cdot Bx(j,1) - \alpha \cdot Ax(j,1)] \cdot \sum_{i=2}^{M+1} [Ax(M+2,i) - B_5 \cdot [Q \cdot Bx(j,1) - \alpha \cdot Ax(j,1)] \cdot \sum_{i=2}^{M+1} [B_3 \cdot Ax(M+2,i) - Ax(1,i)] + B_1 \cdot [Q \cdot Bx(j,M+2) - \alpha \cdot Ax(j,M+2)] \cdot \sum_{i=2}^{M+1} [B_3 \cdot Ax(M+2,i)] - Ax(1,i)\right] \bar{C}_1(i) + B_5 \cdot Pe_L \cdot G \cdot \bar{C}_2|_{j=M+2}[Q \cdot Bx(j,1) - \alpha \cdot Ax(j,1)] - B_1 \cdot Pe_L \cdot G \cdot \bar{C}_2|_{j=M+2}[Q \cdot Bx(j,M+2) - \alpha \cdot Ax(j,M+2)] - m \cdot K \cdot \tau_{fL} \cdot [\bar{C}_1(j) - \bar{q}_1(j)] \qquad (32)$$

Equation 21 can be written as,

$$\frac{d\bar{q}_1}{d\tau}(j) = \tau_{fL}(\bar{C}_1(j) - \bar{q}_1(j)) \quad j = 2, M+1 \qquad (33)$$

In equation 32,

$$B_1 = 1/\{Ax(1,M+2) - [B_3 \cdot Ax(M+2,M+2)]\}$$

$$B_2 = Ax(M+2,M+2)/\{Ax(1,M+2) - [B_3 \cdot Ax(M+2,M+2)]\}$$

$$B_3 = [Ax(1,1) - Pe_L]/Ax(M+2,1)$$

$$B_4 = 1/Ax(M+2,1)$$

$$B_5 = B_2 \cdot B_4$$

$$Q = \alpha/Pe_L$$

Equations 28 and 29 which describe the blowdown operation in bed 2 (step 2) may be combined and reduced to a set of ODE's

$$\frac{d\bar{C}_2}{d\tau}(j) = \left[\sum_{i=2}^{M+1} [P \cdot Bx(j,i) + F(j) \cdot Ax(j,i)] - [D_4 \cdot (P \cdot Bx(j,1) + F(j) \cdot Ax(j,1)) \cdot \sum_{i=2}^{M+1} Ax(M+2,i)] - D_5 \cdot [P \cdot Bx(j,1) + F(j) \cdot Ax(j,1)] \cdot \sum_{i=2}^{M+1} [D_3 \cdot Ax(M+2,i) - Ax(1,i)] + D_1 \cdot [P \cdot Bx(j,M+2) + F(j) \cdot Ax(j,M+2)] \cdot \sum_{i=2}^{M+1} [D_3 \cdot Ax(M+2,i) - Ax(1,i)]\bar{C}_2(i)\right] + [y_D \cdot \bar{C}_2(j)] \qquad (34)$$

Since we have assumed the solid phase concentration to be frozen,

$$\frac{d\bar{q}_2}{d\tau}(j) = 0 \qquad (35)$$

In equation 34,

$$D_1 = 1/\{Ax(1,M+2) - [D_3 \cdot Ax(M+2,M+2)]\}$$

$$D_2 = Ax(M+2,M+2)/\{Ax(1,M+2) - [D_3 \cdot Ax(M+2,M+2)]\}$$

$$D_3 = Ax(1,1)/Ax(M+2,1)$$

$$D_4 = 1/Ax(M+2,1)$$

$$D_5 = D_2 \cdot D_4$$

The dimensionless partial differential equations for the high pressure flow in bed 1 (step 3), the low pressure flow in bed 2 (step 3), and the blowdown of bed 1 (step 4), were similarly written and reduced to sets of ODE's by the orthogonal collocation method. The resulting ODE's were solved using Adam's variable step integration algorithm as provided in the FORSIM package (Atomic Energy of Canada, 1976).

NOTATION

$Ax(j,i)$ = collocation coefficient for gradient, external field
$Bx(j,i)$ = collocation coefficient for Laplacian, external field
C_i = adsorbate concentration in gas phase for bed i, mol/m^3
$\bar{C}_i$ = C_i/C_o (−)
C_o = adsorbate concentration in feed gas, mol/m^3
D_{Li} = axial dispersion coefficient for bed i, m^3/sec
k_i = external film mass transfer coefficient for bed i, s^{-1}
K = adsorption equilibrium constant (−)
L = adsorbent bed length, m
m = $(1-\epsilon)/\epsilon$ (−)
P = total pressure in the column, atm (× 101.3 = kPa)
Pe_H = u_2L/D_{L_2}, Peclet number at high pressure (adsorption) step (−)
Pe_L = u_1L/D_{L_1}, Peclet number at low pressure (desorption) step (−)
P_H = column pressure during adsorption step, atm (× 101.3 = kPa)
P_L = column pressure during desorption step, atm (× 101.3 = kPa)
q_i = adsorbate concentration in solid phase for bed i, mol/m^3
$\bar{q}_i$ = q_i/KC_o (−)
q_i^* = KC_i, mol/m^3
t = time, s
t_B = time for blowdown and repressurization (steps 2 and 4), sec
t^* = time for adsorption and desorption (steps 1 and 3), sec
u = interstitial velocity, m/s
u_i = interstitial velocity for bed i, m/s
U = u/u_2 (−)

x = z/L (−)
z = position in the bed, m
(−) = dimensionless quantity

Greek Letters

α = volumetric purge to feed ratio, u_1/u_2 (−)
ϵ = bed porosity (−)
τ = $u_2 t/L$ (−)
τ_b = $u_2 t_B/L$
τ_{fH} = $k_2 L/u_2$ (−)
τ_{fL} = $k_1 L/u_2$ (−)

LITERATURE CITED

Atomic Energy of Canada, *FORSIM, A Fortran Package for the Automated Solution of Coupled Partial and/or Ordinary Differential Equation Systems*, Atomic Energy of Canada Ltd (1976).

Chan, Y. N., F. B. Hill, and Y. W. Wong, "Equilibrium Theory of a Pressure Swing Adsorption Process," *Chem. Eng. Sci.*, **36**, 243 (1981).

Chihara, K., and M. Suzuki, "Nonisothermal Pressure Swing Adsorption," Presented at 2nd World Cong. Chem. Eng., Montreal (Oct., 1981). See also *J. Chem. Eng.*, Japan **16**, 53 (1983).

Finlayson, B. A., *Method of Weighted Residuals and Variational Principles*, Academic Press, New York (1972).

Knaebel, K. S., and F. B. Hill, "Analysis of Gas Purification by Heatless Adsorption," Paper No. 91d, AIChE Ann. Meet., Los Angeles (Nov., 1982).

Knoblauch, K., "Pressure Swing Air Separation Geared for Small Volume Users," *Chem. Eng.*, **85**(25), 87 (1978).

Mitchell, J. E., and L. H. Shendalman, "Study of Heatless Adsorption in the Model System CO_2 in He. II," *AIChE Symp. Ser.* **69**(134) 25 (1973).

Raghavan, N. S., and D. M. Ruthven, "Numerical Simulation of a Fixed Bed Adsorption Column by the Method of Orthogonal Collocation," *AIChE J.*, **29**(6), 922 (1983).

Santacesaria, E., et al., "Separation of Xylenes on Y Zeolites. 2: Breakthrough Curves and Their Interpretation," *Ind. Eng. Chem. Proc. Des. Dev.*, **21**, 446 (1982).

Shendalman, L. H., and J. E. Mitchell, "A Study of Heatless Adsorption in the Model System CO_2 in He. I," *Chem. Eng. Sci.*, **27**, 1,449 (1972).

Skarstrom, C. W., "Use of Adsorption Phenomena in Automatic Plant-Type Gas Analyzers," *Ann., NY Acad. Sci.*, **72**, 751 (1959).

Skarstrom, C. W., "Fractionating Gas Mixtures by Adsorption," U.S. Patent 2,444,627 (1960), assigned to Esso Research and Eng. Co.

———, "Heatless Fractionation of Gases Over Solid Adsorbents," *Recent Developments in Separation Science*, **2**, 95, CRC Press, Cleveland, OH (1972).

Villadsen, J. V., and W. E. Stewart, "Solution of Boundary-Value Problems by Orthogonal Collocation," *Chem. Eng. Sci.*, 22, 1,483 (1967).

Manuscript received Apr. 1, 1983; revision received Sept. 7, 1983, and accepted Sept. 7.

An NRTL Model for Representation and Prediction of Deviation from Ideality in Electrolyte Solutions Compared to the Models of Chen (1982) and Pitzer (1973)

F. X. BALL, W. FÜRST, and H. RENON

Groupe Commun Réacteurs et Processus
ENSTA-ENSMP Associé au CNRS
75006 Paris, France

A new method of representation of electrolyte solution nonideality is derived, on the basis of similar assumptions, from a model applied by Cruz and Renon (1978) to binary electrolyte solutions. In order to test the validity of the model for representation of strong electrolyte properties, parameters were fitted to osmotic coefficient data for single, completely dissociated salts in aqueous solutions and were used to calculate osmotic coefficients of mixed aqueous electrolytes. Results are compared with those given by Chen's local composition model (Chen et al., 1982; Aspen, 1983) and Pitzer's truncated model (Pitzer, 1973, 1979; Pitzer and Mayorga, 1973; Pitzer and Kim, 1974), the same number of adjustable parameters being used in each case.

The average standard deviations for single electrolytes are within 1% in the case of 1-1 salts for the three models, and within 2% in the other cases, except for Chen's model (5%). As for predicted results, both local-composition models yield standard deviations of less than 2%, while the accuracy given by the Pitzer model is better than 1.5%.

SCOPE

Simple methods for representing deviations from ideality in electrolyte solutions are needed to design industrial processes, especially for transformation of raw materials and pollution control. Many models have been developed for that purpose on the basis of semiempirical extensions of the Debye-Hückel expression for the excess Gibbs energy.

The ion interaction model of Pitzer (1973) has proved especially useful; it yields accurate results for aqueous salt solutions properties up to a six-molal concentration.

Some years ago Cruz and Renon proposed a system of equa-

Correspondence concerning this paper should be addressed to H. Renon.